

Metabolic engineering for provitamin D3 biosynthesis in tomato

Sunghwa Choe (✉ shchoe@snu.ac.kr)

Seoul National University <https://orcid.org/0000-0001-5541-484X>

Sunmee Choi

G+FLAS Life Sciences

Jeongmo Kim

G+FLAS Life Sciences

Jongjin Park

Naturegenic Inc.

Jinhwa Kim

G+FLAS Life Sciences

Article

Keywords: CRISPR-Cas9, Non-GMO, Vegetarian, Vitamin D deficiency, COVID-19

Posted Date: March 28th, 2022

DOI: <https://doi.org/10.21203/rs.3.rs-1403571/v1>

License:  This work is licensed under a Creative Commons Attribution 4.0 International License.

[Read Full License](#)

19 **Providing adequate vitamin D3 for the human diet is a long-standing goal of crop**
20 **breeding because most plants have relatively low levels of this nutrient naturally. Using**
21 **CRISPR-Cas9 editing of the tomato genome, we increased provitamin D3 levels in**
22 **tomato fruits to up to 1 mg per 100 grams dry weight. Use of this provitamin D3 tomato**
23 **could ameliorate widespread vitamin D deficiencies around the world.**

24 In humans, provitamin D3 (ProvitD3) plays dual roles as a protectant against ultraviolet (UV)
25 irradiation in the skin and as a precursor for the biosynthesis of active vitamin D3, an
26 important human steroid hormone. Studies suggest that circulatory vitamin D3 (VitD3) levels
27 in humans around the world are well below desirable levels, especially in those not frequently
28 exposed to substantial sunlight¹. Dietary supply offers a means to ameliorate this shortage.
29 However, only a limited number of animal-derived foods, including fish, egg yolks, and beef
30 liver, contain VitD²; vegetables and fruit are not significant sources of VitD because the
31 biosynthetic activity of plants in the direction of ProvitD3 production is low³. We
32 hypothesized that metabolic engineering of tomato plants, a crop widely cultivated and eaten
33 worldwide, to accumulate ProvitD3 may help ameliorate endemic global VitD deficiencies,
34 especially among people whose options for dietary changes are relatively limited, such as the
35 elderly, vegetarians, and patients with obesity or living in nursing homes and hospitals.

36 ProvitD3 is 7-dehydrocholesterol (7DHC), the penultimate intermediate in the
37 cholesterol biosynthetic pathway. 7DHC is converted to cholesterol by 7DHC reductase⁴. In
38 an alternative branch of this pathway, exposure to UV-B light (290–315 nm) cleaves the bond
39 between the C9 and C10 carbons of 7DHC to yield previtamin D3 (PrevitD3; Fig. 1a).
40 Further enzymatic modification by liver CYP2R1 (Cytochrome P450 Family 2 Subfamily R
41 Member 1) and kidney CYP27B1 solubilizes PrevitD3 to form the active vitamin 1,25-
42 dihydroxy vitamin D (1,25(OH)2D)⁵, which plays diverse roles in human metabolism,
43 including calcium and phosphorus absorption.

44 We hypothesized that knocking out a crop gene homologous to Arabidopsis
45 (*Arabidopsis thaliana*) *DWARF5* (*DWF5*), which encodes sterol 7-reductase, would result in
46 ProvitD3 accumulation in leaves or fruits⁶. An ortholog of Arabidopsis *DWF5* has been
47 identified in humans^{4,7}, and loss-of-function mutations in this gene cause severe growth
48 defects both in plants and in humans⁸. Like Arabidopsis, lettuce (*Lactuca sativa*) has a single
49 copy of this gene (*LsDWF5*) and a gene organization comprising 13 exons (Fig. 1b). To
50 metabolically engineer lettuce for ProvitD accumulation, we selected appropriate single guide
51 RNAs (sgRNAs) and introduced *LsDWF5* loss-of-function mutations into lettuce through
52 clustered regularly interspaced short palindromic repeats (CRISPR)-CRISPR-associated
53 nuclease (Cas9)-mediated genome editing (Extended Data Fig. 1a). We obtained 13 lines with
54 characteristic insertion or deletion (InDel) mutations (Fig. 1c). Comparing mutant #13-17 (T₁
55 generation descendant of lettuce T₀ mutant #13) to wild-type plants indicated that, like its
56 Arabidopsis counterpart, the lettuce *Lsdwf5* mutant showed dwarfism with small leaves (Fig.
57 1d; Extended Data Fig. 2 and 3).

58 To increase ProvitD3 levels while maintaining overall plant architecture and without
59 compromising growth, an agriculturally desirable trait, we looked for a crop plant with at
60 least two functionally redundant *DWF5* copies. Tomato (*Solanum lycopersicum*) has two
61 copies of the gene, *SIDWF5-1* and *SIDWF5-2*, which are both structurally similar to the
62 Arabidopsis and lettuce genes (Fig. 2a,b) and also known for active biosynthesis of
63 cholesterol as well as campesterol⁹. We established that *SIDWF5-1* is preferentially expressed

64 in fruits, whereas *SIDWF5-2* was relatively weakly expressed (Fig. 2c). We hypothesized that
65 knocking out *SIDWF5-1* could thus be a good strategy to increase ProvitD3 levels with
66 relatively minimal effects on plant architecture. When we aligned the DNA sequences of
67 exon 6 in the two *SIDWF5* genes, we were able to identify two potential sgRNAs targeting
68 only the *SIDWF5-1* gene (Fig. 2d). We placed these two closely located sgRNAs sequences
69 31 bases apart under the control of the promoter from the Arabidopsis small nucleolar RNA
70 *U6* and then transformed the resulting Cas9 constructs into tomato hypocotyl tissue derived
71 from 6-day-old tomato seedlings (Extended Data Fig. 1b and 3e through h). Sixteen
72 transgenic seedlings regenerated after transformation (T_0 generation); our examination of the
73 editing events in these seedlings showed that 14 out of 16 carried InDel mutations in at least
74 one of the two sgRNA sites on on-target (Fig. 2d; Extended Data Fig. 3 and 4; Supplementary
75 Table 1). Further targeted deep-se analysis with the DNA prepared from T_2 lines revealed
76 homozygosity for the InDel mutations (Supplementary Table 2). Frequency of InDel
77 mutations at off-target sites was not significant except sgRNA_S12-OT1 site in #3-14 line
78 (Supplementary Table 3), which is located at *SIDWF5-2*.

79 Next, we collected fruits and harvested T_1 seeds from seven of the 14 mutant plants.
80 To obtain lines that are transgene free but carry the desired mutations, we plated 28–30 T_1
81 seeds for each line and tested whether the selection marker, conferring hygromycin
82 resistance, remained in the genome or had segregated out. Two plants derived from #3-14-2
83 and #7-1-24 lines were free of the transgene and displayed vigor indistinguishable from that
84 of wild-type plants (Fig. 2e). We examined the ProvitD3 levels in the offspring plants of #3-
85 14 and #7-1 segregating for mutations in *SIDWF5-1* by liquid chromatography–tandem mass
86 spectrometry (LC-MS/MS; Fig. 2f). Whereas ProvitD3 was undetectable in wild-type plants,
87 the mature fruits from the two mutant lines showed levels ranging from 117 to 1,026 mcg per
88 100 g dry weight, although these were much lower in leaves and stems (Fig. 2g). When
89 converted to fresh weight equivalents, this would equate to up to 10–100 mcg ProvitD3 per
90 medium-sized tomato fruit of 140 g fresh weight, about half the fruit of beefsteak tomatoes.
91 Thus, we have created a version of tomato—already recognized as a 'superfood' for its high
92 content of other vitamins and antioxidants—further fortified to contain sufficient ProvitD3 to
93 meaningfully improve human vitamin D intake.

94 The US National Institute of Health (NIH) recommends maintaining serum 25-
95 hydroxyvitamin D [25(OH)D] concentrations of 50 nmol/L, but the majority of people have
96 lower levels. Thus, taking daily supplements containing 10–20 mcg vitamin D is
97 recommended (<https://ods.od.nih.gov/factsheets/VitaminD-HealthProfessional/>). Our data
98 suggest that this recommendation could be met by eating one of our tomato fruits each day.
99 Thus, through CRISPR-Cas9 genome editing of a widely used crop plant, we have created a
100 new variety with the potential to improve human dietary ProvitD3 intake via ingestion of a
101 sustainable, plant-derived food that is already widely consumed globally, and thereby
102 alleviate VitD deficiency worldwide.

103

104 **Methods**

105 **Vector construction**

106 A construct used for *Agrobacterium* (*Agrobacterium tumefaciens*)–mediated genetic transformation
107 was created harboring an antibiotic selection cassette, the *Cas9* gene, and tandem polycistronic tRNA-

108 gRNA repeats for positive selection on both kanamycin and hygromycin and genome editing. The
109 human-codon-optimized *Cas9* gene originated from *Streptococcus pyogenes* (SpyCas9) was cloned
110 into the pCAMBIA1300 plasmid (#44183; Addgene) and placed under the control of the Arabidopsis
111 *Ubiquitin 10* promoter. To facilitate nuclear localization of the Cas9 protein in tomato cells, simian
112 vacuolating virus 40 (SV40 NLS) and bipartite nuclear localization signals (BPNLSs) were added at
113 the N and C termini of Cas9. Using the BsaI restriction enzyme, two sgRNAs were inserted into the
114 pCAMBIA-Cas9 backbone and driven by the promoter of the Arabidopsis small nucleolar *U6* RNA.

115

116 **Lettuce transformation and regeneration**

117 One-week-old cotyledons of lettuce (*Lactuca sativa* cv. Hanbat Cheongchima) were cut into ~1-cm²
118 pieces and co-cultured with Agrobacterium strain GV3101 (OD₆₀₀ = 0.6) harboring the *Cas9* construct
119 for 2 days at 25°C in the dark. The co-cultured cotyledons were transferred to a callus-inducing
120 medium, consisting of Murashige and Skoog (MS) medium (M0221, Duchefa Farma B.V) with 0.1
121 mg/L β-benzylaminopurine (BAP, D130, Phytotech Labs), 0.1 mg/L α-naphthalene acetic acid (NAA,
122 N600, Phytotech Labs), 7% (w/v) plant agar (P1001, Duchefa), and 30 g/L sucrose (S0809, Duchefa),
123 and grown at 25°C in the light for 2 days. To select transformed tissues, the MS-grown cotyledons
124 were transferred to MS medium containing 5 mg/L DL-phosphinothricin (BASTA, MB-P4691,
125 MBcell) and 200 mg/L ticarcillin disodium (T1090, Duchefa) and grown at 25°C in the light for a
126 further 6–8 weeks, with the growth plates replaced by fresh plates at 2-week intervals until shoot
127 generation occurred. The emerging shoots were transferred to full-strength MS medium and grown
128 into rooted plantlets in containers. The plantlets were transferred to soil-filled pots and maintained
129 until seed harvest.

130 **Tomato transformation and regeneration**

131 Two-week-old hypocotyls of tomato (*Solanum lycopersicum* cv. Seogwang) were cut into
132 approximately 1-cm² pieces and co-cultured with Agrobacterium strain LBA4404 (OD₆₀₀ = 0.5)
133 harboring the *Cas9* construct for 2 days at 25°C in the dark. The co-cultured hypocotyls were
134 transferred to callus-inducing medium (MST) consisting of full-strength MS medium (M0221,
135 Duchefa Farma B.V.) containing 0.5 mg/L nicotinic acid (1414-0130, Showa), 100 mg/L myoinositol
136 (MB-I4715, MB cell), 0.5 mg/L pyridoxine HCl (P-8666, Sigma), 0.1 mg/L thiamine HCl (T0614,
137 Duchefa), 30 g/L sucrose (S0809, Duchefa Farma B.V), 0.25% (w/v) Gelrite (71015-52-1, Duchefa)]
138 with 0.1 mg/L NAA (N600, Phytotech Labs), and 1 mg/L BAP (D130, Phytotech Labs) and grown at
139 25°C in the light for 2 days.

140 To select transformed tissues, the MST-grown hypocotyls were transferred to full-strength
141 MST medium containing 2 mg/L zeatin (Z860, Phytotechlab), 0.2 mg/L indole-3-acetic acid (IAA,
142 I0901, Duchefa Farma B.V.), 25 mg/L hygromycin B (LPS solution, HYB01), and 200 mg/L
143 ticarcillin disodium (T1090; Duchefa Farma B.V.) and grown at 25°C in the light for 8–12 weeks. The
144 growth plates were replaced by fresh plates at 2-week intervals until shoot generation occurred. The
145 emerging shoots were transferred to half-strength MST medium with 0.2 mg/L IAA and grown into
146 rooted plantlets in containers. The plantlets were transferred to soil-filled pots and maintained until
147 seed harvest.

148

149 **Reverse-transcription quantitative PCR (RT-qPCR)**

150 Total RNA was isolated from plant tissues using the RNeasy® plant mini kit (#74904, Qiagen, Hilden,
151 Germany). Reverse transcription was performed with a RevertAid RT Reverse Transcription Kit
152 (K1691; Thermo Fisher Scientific, Waltham, MA, USA) using 3 µg of total RNA and was followed by
153 qPCR analysis of the resulting first-strand cDNA. The primers used for qPCR are listed in

154 Supplementary Table 5. RT-qPCR was performed in 96-well blocks with a Real-Time PCR System
155 (4379216; Applied Biosystems, Foster City, CA, USA) using the KAPA SYBR® FAST qPCR Master
156 Mix Kit (KK4601; KAPA Biosystems, Wilmington, MA, USA) in a volume of 20 µL. The reactions
157 were performed in three technical repeats per run, and three biological replicates were included.
158 Absolute quantification was performed using standard curves generated by amplification of a diluted
159 series of cDNA containing individual transcripts. The transcript levels of each gene in different
160 samples were normalized to an internal control, *ACTIN* (Solyc11g005330.2), using the $2^{-\Delta\Delta CT}$ method.

161

162 **T7E1 assay**

163 Genomic DNA was isolated from transgenic plants using the DNeasy Plant Mini Kit (#69104,
164 Qiagen). The target DNA region was amplified and subjected to the T7E1 assay as described
165 previously (Woo et al., 2015). For heteroduplex formation, PCR products were denatured at 95°C for
166 10 min and subjected to an annealing program of 95°C to 85°C (-2°C/sec) followed by a 85°C to
167 25°C (-0.1°C/sec) slow cooldown using a thermal cycler. Annealed PCR products were incubated
168 with T7 endonuclease I (#m0302, NEB) at 37°C for 20 min and analyzed via agarose gel
169 electrophoresis.

170

171 **Sanger sequencing of target regions**

172 The sgRNA target regions were amplified from genomic DNA using Q5 Polymerase (#M0491; New
173 England Biolabs) in a 25-µL reaction volume. Then, the PCR products were cloned into a 3'-end T-
174 tailed vector using a PCR Cloning Kit (VT201-020; Biofact Pharma Ltd., Kildare, Ireland). Finally,
175 20 clones for each sample were individually sequenced. The primers used for on-target site mutation
176 analysis are listed in Supplementary Table 4 (lettuce) and 6 (tomato).

177

178 **Targeted deep sequencing**

179 To compare editing events in the target loci, on-target sequencing was performed for the 23 lines of
180 the T₁ generation, 21 lines of the T₂ generation, and the sequences compared to that of the wild type
181 (Supplementary Table 1 and 2). The targeted primers were designed from genomic DNA (1st PCR,
182 Supplementary Table 6). Sequencing adaptors were added for the amplicon PCR (Supplementary
183 Table 6). High-throughput sequencing was performed using the MiniSeq System (SY-420-1001;
184 Illumina, Inc., San Diego, CA, USA) and analyzed using methods available online¹⁰.

185

186 **Off-target deep sequencing**

187

188 **The comparison target for off-target sequencing is seedling of T1 generation #3-14 and #7-1**
189 **were used and compared with wild type. Potential off-target sites were identified in the *S.***
190 ***lycopersicum* genome using the Cas-OFFinder (<http://www.rgenome.net/cas-offinder>)**
191 **algorithm. The Sol Genomics Network (<https://solgenomics.net>) was used as the reference**
192 **genome to identify homologous sequences that differed from the on-target sequences by up to 4**
193 **nt. Of a total of 32 sites, 11 were selected for targeted deep sequencing. The primers for the on-**
194 **target and potential off-target sites were designed from genomic DNA (1st PCR, supplementary**
195 **Table 7). Sequencing adaptors were added for the 2nd PCR (supplementary Table 7). High-**
196 **throughput sequencing was performed using the MiniSeq System (SY-420-1001; Illumina, Inc.,**
197 **San Diego, CA, USA).**

198

199 **Authentic chemical standards.**

200 7-Dehydrocholesterol (ProvitD3), a 5,7-conjugated diene sterol, is a biosynthetic precursor of
201 cholesterol. Approximately 5 mg of 7-dehydrocholesterol (purity \geq 95%, #30800, Sigma-Aldrich,
202 Germany) was weighed, and 50 mL of methanol was added to result in a concentration of 100
203 mcg/mL. The sterol was then dissolved by sonication. The stock solution was diluted appropriately
204 with methanol to produce standard solutions at concentrations of 70, 140, 280, 560, and 1120 ng/mL.
205 The standard solutions were run under the same conditions as the test samples (see below), and the
206 resulting data were used to prepare standard curves and a coherent calculation formula. The results for
207 the test samples were then extrapolated from the standard curve to determine relative concentrations
208 of 7-DHC in the fruit samples.

209

210 **Sample preparation**

211 Samples from the T₂ generations of #3-14 (four individual lines) and #7-1 (11 individual lines) as well
212 as wild-type (WT) plants were compared. To prepare analytic samples, 15 fruits were picked and
213 weighed to obtain an average 140 g fresh weight per fruit. When the fresh fruits were freeze dried,
214 about 7% of the original fresh weight remained. To approximately 1 g (dry weight) of each fruit
215 sample placed in a flask, 30 mL of ethanol and 1 mL of 10% (v/v) ethanolic pyrogallol were added.
216 Then, 3 mL of 90% (w/v) potassium hydroxide (#484016, Sigma-Aldrich) was added, and each
217 mixture was incubated for 30 min with repeated vortexing every 10 min in an 80°C water bath. After
218 cooling down to room temperature, 30 mL each of distilled water and *n*-hexane were added and the
219 mixture was shaken for 1 h. The upper layer (hexane) was transferred to a separatory funnel, and
220 another 30 mL of *n*-hexane was added to the water layer and mixed by vortexing. The upper layer was
221 again pooled into the separatory funnel. 100 mL of distilled water was used twice for washing the
222 hexane layer. Then, the hexane layer was dehydrated with anhydrous sodium sulfate, concentrated,
223 dissolved in 5 mL methanol, and the filtered through a polytetrafluoroethylene (PTFE) syringe filter
224 (CLS431227, Merck) to prepare test solutions.

225

226 **LC-MS/MS analysis of ProvitD3**

227 The prepared samples were analyzed by LC-MS/MS (using a UHPLC TSQ Quantis™, Thermo
228 Scientific) at the Korea Health Supplements Institute (<http://www.khsi.re.kr>). Sample analysis was
229 carried out using two isocratic solvents. Liquid chromatography was performed with Waters HSS
230 T3(2.1 × 100 mm with 1.8 μm of particle size) column. The mobile phase consisted of two solvents
231 (A) 0.1% formic acid in distilled water, and (B) 0.1% formic acid in methanol, and the separation was
232 performed using the following gradient of A–B: 0 min (90:10, v/v), 1 min (0:100, v/v), 10 min (0:100,
233 v/v), 10.1 min (90:10, v/v), and 14 min (90:10, v/v) at a flow-rate of 0.2 ml/min. The injection
234 volume was 20 μL. MS/MS data for 7-DHC were acquired in positive-ion mode using atmospheric
235 pressure chemical ionization (APCI) and selected reaction monitoring (SRM); a parent ion mass of
236 385.275 and product ion masses of 367.437, 201.315, and 241.325 were used for limit of detection
237 (LOD) determination. MS parameters were optimized for 7-DHC and were as follows: Auxiliary gas
238 pressure was set at 1/5 pressure level of the sheath gas, and nitrogen was utilized for both. The
239 positive-ion discharge current was set to 4 μA, and the ion transfer tube temperature was set at 325°C.

240

241 **Data availability**

242 **Acknowledgments**

243 This project was supported by the CRISPR PLUS R&D program (2019GFRND-GFC102)
244 supported by G+FLAS Life Sciences, Inc.

245

246 **Author contributions**

247 S.Cho designed and supervised the research, and wrote the article. S.Choi, Jinhwa K.,
248 Jeongmo K., and J.P. performed the research and prepared the figures and tables.

249

250 **Competing financial interests**

251 S.Cho is a founder of the two biotech companies, G+FLAS Life Sciences, Inc. and
252 Naturegenic Inc. S.Choi, Ji.K., and Je.K. are employees of G+FLAS Life Sciences. J.P. is an
253 employee of Naturegenic Inc. Authors are inventors on a patent application covering the
254 genome editing method for plant-based vitamin D3 production described in this manuscript.
255

256 **Additional information**

257 Supplementary information is available for this paper at [https://....](https://...) . Correspondence and
258 requests for materials should be addressed to S.C.

259

References

- 260 1 Cashman, K. D. *et al.* Vitamin D deficiency in Europe: pandemic? *Am J Clin Nutr* **103**, 1033-1044,
261 doi:10.3945/ajcn.115.120873 (2016).
- 262 2 Schmid, A. & Walther, B. Natural vitamin D content in animal products. *Adv Nutr* **4**, 453-462,
263 doi:10.3945/an.113.003780 (2013).
- 264 3 Japelt, R. B. & Jakobsen, J. Vitamin D in plants: a review of occurrence, analysis, and biosynthesis. *Front*
265 *Plant Sci* **4**, 136, doi:10.3389/fpls.2013.00136 (2013).
- 266 4 Wassif, C. A. *et al.* Mutations in the human sterol delta7-reductase gene at 11q12-13 cause Smith-Lemli-
267 Opitz syndrome. *Am J Hum Genet* **63**, 55-62, doi:10.1086/301936 (1998).
- 268 5 Saponaro, F., Saba, A. & Zucchi, R. An Update on Vitamin D Metabolism. *Int J Mol Sci* **21**,
269 doi:10.3390/ijms21186573 (2020).
- 270 6 Silvestro, D. *et al.* Vitamin D5 in Arabidopsis thaliana. *Sci Rep* **8**, 16348, doi:10.1038/s41598-018-
271 34775-z (2018).
- 272 7 Lecain, E., Chenivresse, X., Spagnoli, R. & Pompon, D. Cloning by metabolic interference in yeast and
273 enzymatic characterization of Arabidopsis thaliana sterol delta 7-reductase. *J Biol Chem* **271**, 10866-
274 10873, doi:10.1074/jbc.271.18.10866 (1996).
- 275 8 Choe, S. *et al.* Lesions in the sterol delta reductase gene of Arabidopsis cause dwarfism due to a block in
276 brassinosteroid biosynthesis. *Plant J* **21**, 431-443, doi:10.1046/j.1365-313x.2000.00693.x (2000).
- 277 9 Kim, T. W. *et al.* Novel biosynthetic pathway of castasterone from cholesterol in tomato. *Plant Physiol*
278 **135**, 1231-1242, doi:10.1104/pp.104.043588 (2004).
- 279 10 Park, J., Lim, K., Kim, J. S. & Bae, S. Cas-analyzer: an online tool for assessing genome editing results
280 using NGS data. *Bioinformatics* **33**, 286-288, doi:10.1093/bioinformatics/btw561 (2017).

281

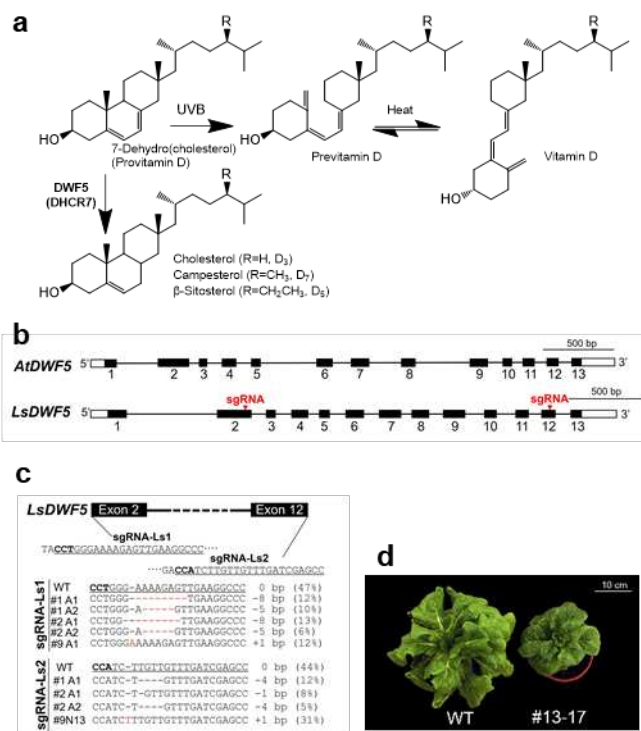
282 **Figure legends**

283

284 **Figure 1 | Provitamin D3 pathway and CRISPR-Cas9 genome engineering of lettuce for**
 285 **VitD production.** **a**, VitD biosynthetic pathway. The final step in sterol biosynthetic
 286 pathways is mediated by plant DWF5 and human DHCR7. Different 7-dehydrosterols
 287 varying at the R group lead to vitamin D3 from 7-dehydrocholesterol, D5 from 7-
 288 dehydrositosterol, and D7 from 7-dehydrocampesterol. VitD5 and VitD7 are more commonly
 289 produced in plants than VitD3. **b**, Gene organization of *DWF5* from *Arabidopsis thaliana*
 290 (*At1g50430*) and *Lactuca sativa* (*LOC111910394*). Open rectangles, untranslated sequences;
 291 filled rectangles, exons; connecting lines, introns; red arrows, locations of single guide RNAs
 292 (sgRNAs). **c**, Mutations introduced by CRISPR-Cas9 genome editing: targeted Sanger
 293 sequencing results of *LsDWF5* in genome-edited mutant plants at the T₀ generation. DNA
 294 prepared from the pooled tissues of T₀ plants were sequenced to find InDel mutations.
 295 Underlined bold letters, PAM sites; red dashed lines, deleted nucleotides; red letters,
 296 insertions. Numbers with plus/minus signs indicate deletions (-) and insertions (+). Numbers
 297 in brackets show frequency of the specific alleles out of 69 T₀ plants for the sgRNA-Ls1 site
 298 and 74 T₀ plants for the sgRNA-Ls2 site. **d**, Phenotypes of a wild-type and an
 299 *Lsdwf5* mutant (#13-17) plant, the latter showing a dwarf phenotype. #13 at T₀ showed
 300 heterozygous mutation of single-base insertion at the sgRNA-Ls2 site, and the offspring #13-
 301 17 has a homozygous mutation.

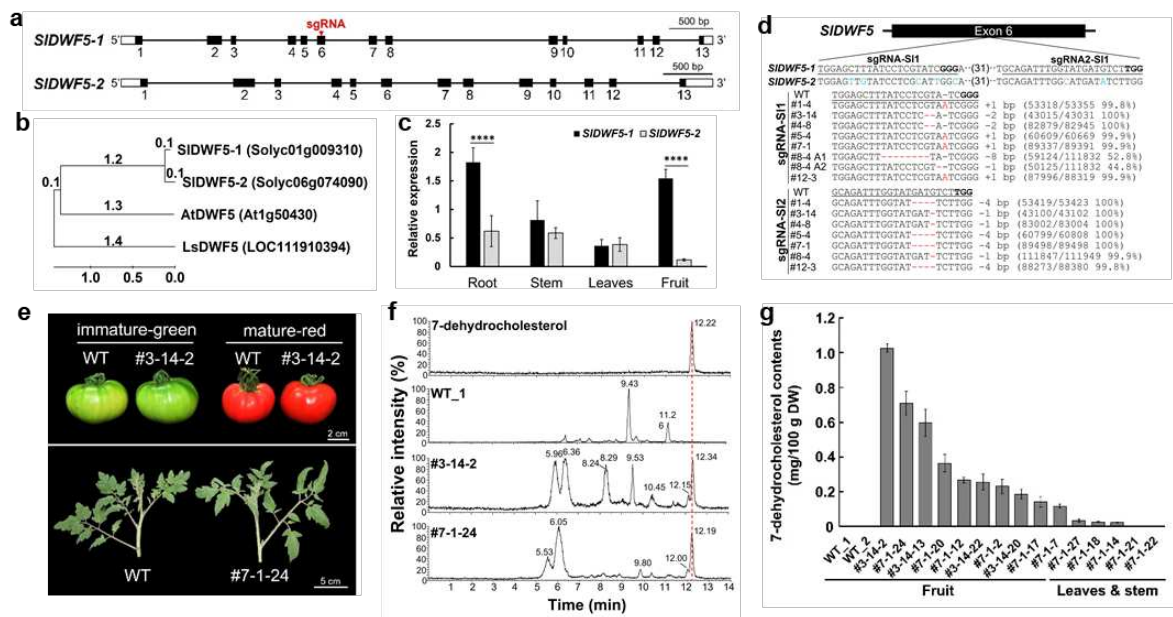
302

303



304

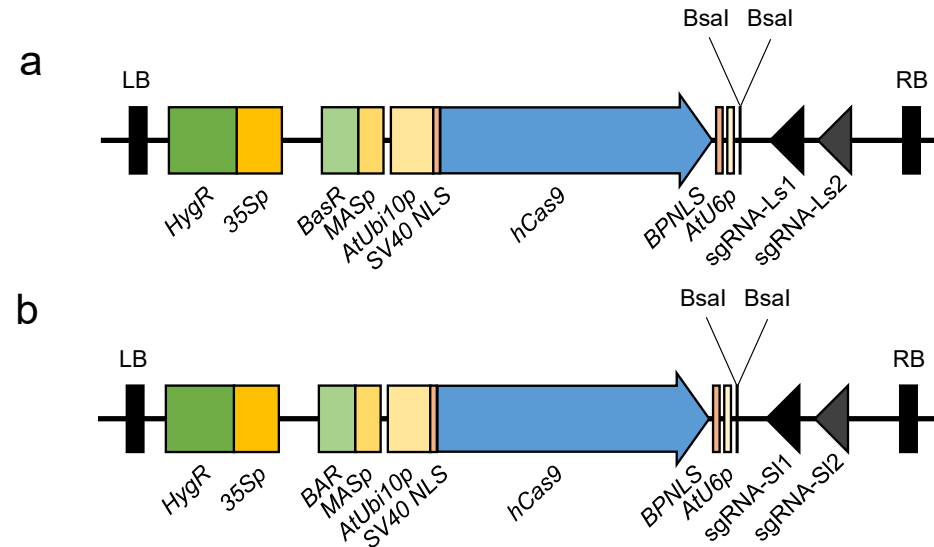
305 **Figure 2 | Provitamin D3 accumulation in genome-edited tomato plants.** a, Schematic
 306 diagram of the *Solanum lycopersicum* *DWF5* genes *SIDWF5-1* (Solyc01g009310) and
 307 *SIDWF5-2* (Solyc06g074090). Open rectangles, untranslated sequences; filled rectangles,
 308 translated exons; connecting lines, introns; red arrow, position of sgRNA. b, Phylogenetic
 309 tree showing the relationship among Arabidopsis *DWF5* and its tomato and lettuce homologs.
 310 Scale indicates relative rate of amino acid substitutions per residue. c, Spatial expression
 311 patterns of the two *SIDWF5* genes determined by reverse-transcription quantitative PCR (RT-
 312 qPCR). All tissues were collected from 8-week-old plants, except for the mature fruits.
 313 Relative expression levels are normalized to those of the tomato actin gene (*ACT1*,
 314 TC194780a). Error bars, s.d. ($n = 3$ biological samples). **** $P < 0.0001$ based on Student's *t*-
 315 test. d, Results of targeted deep sequencing of T₁ plants at *SIDWF5-1*. Genotypes of *SIDWF5-1*
 316 mutants were confirmed by Illumina Mini-Seq. Underlined boldface, PAM site; red dashed
 317 lines, deleted nucleotides; red letters, inserted bases. Numbers with plus/minus signs indicate
 318 deletions (-) and insertions (+). Numbers in parentheses shows frequency of the specific
 319 mutations after targeted deep sequencing reads. e, Little phenotypic difference was found
 320 between *Sldwf5-1* mutants and the wild type (WT). Immature green and mature red fruits of
 321 the WT and *Sldwf5-1* mutants (#3-14-2) after 6 months of growth showed no significant
 322 difference in shape or size. The stem node of one *Sldwf5-1* mutant (#7-1-24) grew by one
 323 fewer node than the WT. f, LC-MS/MS spectra showing ProvitD3 peaks relative to the
 324 ProvitD3 (7-dehydrocholesterol) standard, in WT fruits (WT_1), and *Sldwf5-1* mutant fruits
 325 (#3-14-2, #7-1-24). Retention time is represented by a red dashed line. g, Concentrations of
 326 ProvitD3 in tissues of T₂ plants of *Sldwf5-1* mutant lines. Error bars, s.d. ($n = 3$ biological
 327 samples).



329

330

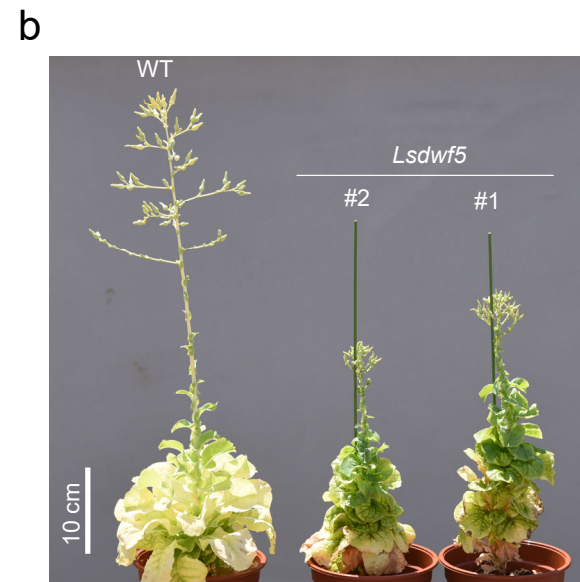
Extended Data Figures and Supplementary Tables



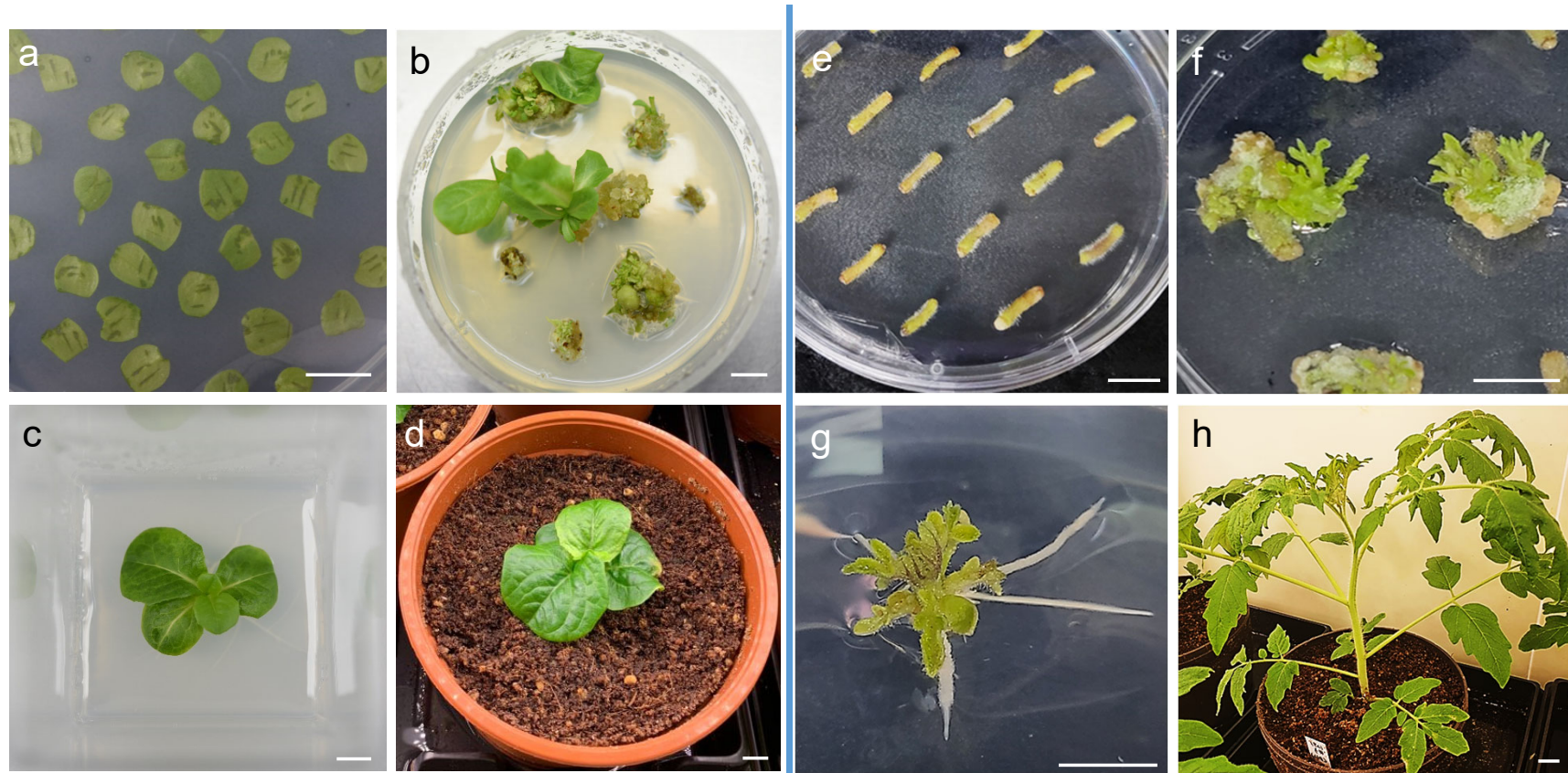
Extended Data Fig. 1. Schematic of the genome-editing binary vector containing two sgRNAs with a gRNA-tRNA linker system. Two sgRNAs were constructed with tandemly arrayed tRNA-spacer 20 bp-sgRNA scaffold systems. Two tandem repeats were placed under the control of a U6 promoter. LB is for the left border sequence of *Agrobacterium* T-DNA, HygR for the coding sequence of the hygromycin B phosphotransferase gene, 35Sp for the cauliflower 35S promoter, BAR for the coding sequence of the BASTA resistance gene phosphinothricin acetyltransferase, MASp for the mannopine synthase (MAS) promoter, AtUbi10p for the *Arabidopsis* ubiquitin 10 gene promoter, SV40 NLS for the nuclear localization signal sequence from simian vacuolating virus 40, hCas9 for the human codon-optimized Cas9 coding sequence, BP-NLS for the bipartite nuclear localization sequence, AtU6p for the *Arabidopsis* U6 gene promoter, two sgRNA for the spacer sequences, the gRNA scaffold for the scaffold sequence for sgRNA, tRNA for the tRNA scaffold for RNase P processing, and RB for the right border.

a

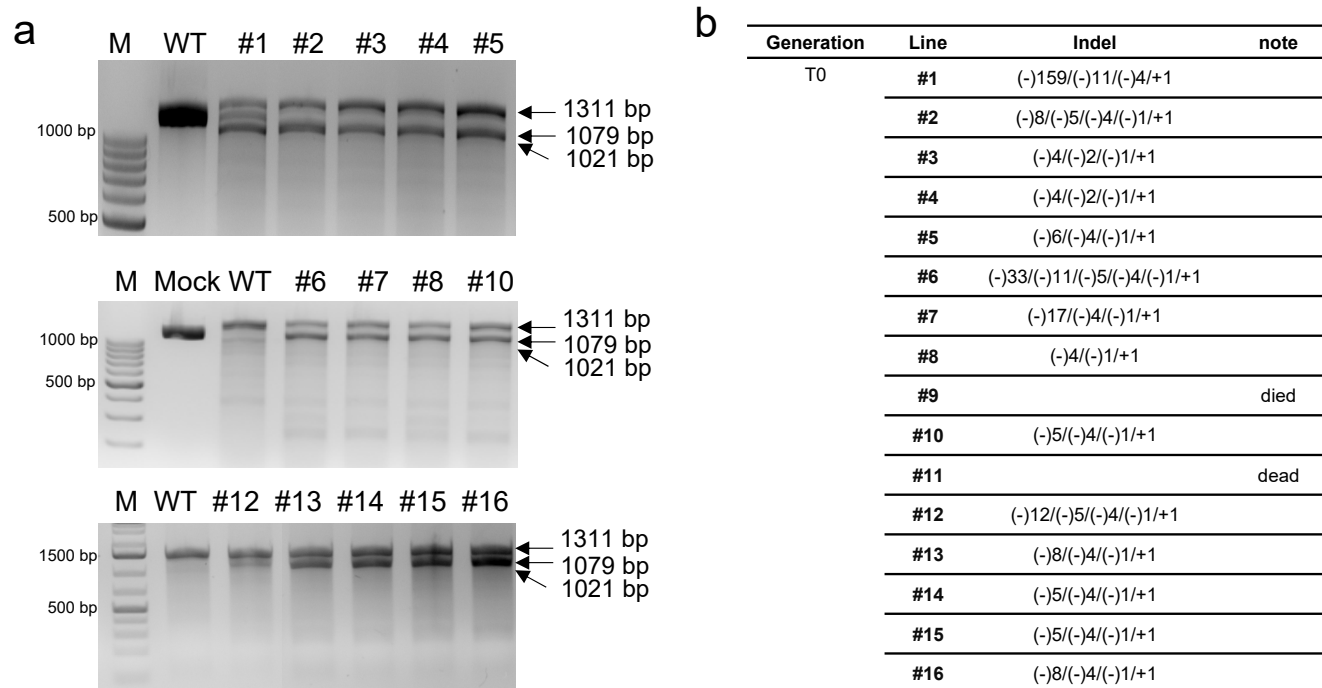
Generation	Line	Indel	note
T0	#1	(-)4/(-)5/(-)8/WT	small amount of seeds
	#2	(-)1/(-)4/(-)5/(-)8/WT	small amount of seeds
	#3	WT	
	#4	(-)5/(-)10/(-)38	died
	#5	(-)8/WT	sterile
	#6	(-)5/(-)8/WT	sterile
	#7	(-)8/(-)195/WT	sterile
	#8	WT	
	#9	+1/+1	sterile
	#10	(-)2/(-)14/WT	small amount of seeds
	#11	WT	
	#12	(-)2/WT	small amount of seeds
	#13	+1/WT	normal amount seeds
	#14	(-)2/(-)5/(-)14/WT	sterile



Extended Data Fig. 2. Detection of gene editing events in transgenic lettuce plants. **a**, Gene editing results by sanger sequencing. Gene editing was confirmed in 11 out of 14 transgenic plants. #4 transgenic plants died during growth. #5, #6, #7, #9 and #14 lines were sterile. **b**, *Lsdwf5* showed dwarfism, short-round leaves and reduced seed setting, or a few seeds, if any.



Extended Data Fig. 3. Plants regenerated after genome editing in *Lactuca sativa* (a-d) and *Solanum lycopersicum* (e-h). **a**, Cotyledons after cocultivation with *Agrobacterium* (GV3101). **b**, Shoots from eight-week-old explants under 5 mg/L BASTA. **c**, Roots from four-week-old explants. **d**, A transgenic lettuce plant. **e**, Hypocotyls after co-cultivation with *Agrobacterium* (LBA4404). **f**, Shoots from ten-week-old explants under 25 mg/L hygromycin. **g**, Roots from four-week-old explants. **h**, A transgenic tomato plant in soil. White scale bars, 1 cm.



Extended Data Fig. 4. Confirmation of gene editing events in tomato transgenic plants by T7E1 assay (**a**) and Sanger sequencing (**b**). **a**, Results of T7E1 analysis on 16 transgenic plants (T0). Confirm that gene editing has occurred in all individual plant. M; Size maker, Mock; no treatment T7Endonuclease 1, WT; Wild type. Treatment of PCR product with 1,311 bp length with T7E1 is cut into 1,079 and 232 for sgRNA_Ls1, and 1,021 and 290 for sgRNA_Ls2. **b**, Gene editing results by Sanger sequencing. Gene editing was confirmed in 14 out of 16 transgenic plants. #9 and #11 transgenic plants died during growth.

Supplementary Table

Table S1. Targeted deep-sequencing to confirm homozygosity for the InDel mutations. DNAs prepared from the select T1 generation of *Sldwf5-1* mutants were subject to Illumina Mini-Seq.

T0 plant No.	T1 plant No.	Total reads (raw fastq)	sgRNA_S11			Total reads (raw fastq)	sgRNA_S12		
			Insertions	Deletions	Indel frequency(%)		Insertions	Deletions	Indel frequency(%)
#1	#1-1	86818	86370	340	86710 (99.8%)	86957	0	86913	86913 (99.9%)
	#1-2	54277	53495	29	53524 (99.9%)	53645	0	53629	53629 (100.0%)
	#1-4	53415	55318	51	53369 (99.8%)	53423	0	53419	53419 (100.0%)
	#1-5	68709	68498	167	68665 (99.9%)	68855	0	68821	68821 (100.0%)
#3	#3-5	50317	44	50256	50300 (99.9%)	50401	0	50376	50376 (100.0%)
	#3-6	70729	70528	65	70593 (99.8%)	70792	0	70775	70775 (99.9%)
	#3-11	54564	17	54531	54548 (100.0%)	54615	0	54615	54615 (100.0%)
	#3-14	43035	16	43015	43031 (100.0%)	43102	0	43100	43100 (100.0%)
	#3-15	53598	53473	70	53543 (99.9%)	53663	0	53663	53663 (100.0%)
	#3-18	52997	49	52868	52917 (99.8%)	52978	0	52978	52978 (100.0%)
#4	#4-4	83111	386	82710	83096 (100.0%)	82938	0	82938	82938 (100.0%)
	#4-8	82901	65	82814	82879 (100.0%)	83004	0	83002	83002 (100.0%)
	#4-9	78655	108	78516	78624 (100.0%)	78519	0	78519	78519 (100.0%)
#5	#5-4	60669	60609	60	60669 (99.9%)	60808	0	60799	60799 (100.0%)
	#5-9	70656	70473	134	70607 (99.9%)	70750	0	70699	70699 (99.9%)
#7	#7-1	89457	89337	54	89391(99.9%)	89541	0	89498	89498 (100.0%)
	#7-5	98801	58	98701	98759 (100.0%)	98838	0	98803	98803 (100.0%)
#8	#8-1	71913	37	39	76 (0.1%)	71691	0	71658	71658 (100.0%)
	#8-3	75821	75656	81	75737 (99.9%)	75901	0	75867	75867 (100.0%)
	#8-4	111832	156	111676	111832 (100.0%)	111849	0	111847	111847 (100.0%)
#12	#12-3	88259	87996	163	88159 (99.9%)	88452	0	88273	88273 (99.8%)
	#12-7	109897	109131	623	109754 (99.9%)	109974	0	109946	109946 (100.0%)
	#12-8	7402	7377	13	7390 (99.8%)	7421	0	7412	7412 (99.9%)

Supplementary Table

Table S2. Targeted deep-sequencing to confirm homozygosity for the InDel mutations. DNAs prepared from the select T2 generation of *Sldwf5-1* mutants were subject to Illumina Mini-Seq.

T2 plant No.	Total reads (raw fastq)	sgRNA_S1			Total reads (raw fastq)	sgRNA_S2		
		Insertions	Deletions	Indel frequency(%)		Insertions	Deletions	Indel frequency(%)
#3-14-1	15202	428	14774	15202 (100.0%)	15179	0	15179	15179 (100.0%)
#3-14-2	9996	15	9977	9992 (100.0%)	10446	0	10446	10446 (100.0%)
#3-14-6	15009	758	14233	14991 (99.9%)	15014	0	14995	14995 (99.9%)
#3-14-13	6601	15	6586	6601 (100.0%)	6735	0	6735	6735 (100.0%)
#3-14-20	3319	10	3309	3319 (100.0%)	3905	0	3905	3905 (100.0%)
#3-14-22	1973	7	1966	1973 (100.0%)	2406	0	2406	2406 (100.0%)
#3-14-29	9791	351	9440	9791 (100.0%)	9795	0	9795	9795 (100.0%)
#7-1-1	16711	16654	37	16691 (99.9%)	16839	0	16828	16828 (99.9%)
#7-1-2	6741	6734	5	6739 (100.0%)	7096	0	7096	7096 (100.0%)
#7-1-3	14058	14033	15	14048 (99.9%)	14057	0	14057	14057 (100.0%)
#7-1-7	7950	7940	2	7942 (99.9%)	8335	0	8335	8335 (100.0%)
#7-1-12	8018	8014	2	8016 (100.0%)	8295	0	8295	8295 (100.0%)
#7-1-14	23130	23117	8	23125 (100.0%)	23204	0	23204	23204 (100.0%)
#7-1-15	20284	20238	26	20264 (99.9%)	20403	0	20403	20403 (100.0%)
#7-1-17	11392	11379	4	11383 (99.9%)	12154	0	12154	12154 (100.0%)
#7-1-18	9984	9979	5	9984 (100.0%)	10080	0	10080	10080 (100.0%)
#7-1-20	7658	7652	0	7652 (99.9%)	8136	0	8136	8136 (100.0%)
#7-1-21	5348	5348	0	5348 (100.0%)	5670	0	5670	5670 (100.0%)
#7-1-22	7719	7711	2	7713 (99.9%)	8139	0	8136	8136 (100.0%)
#7-1-24	6645	6625	18	6643 (100.0%)	6728	0	6728	6728 (100.0%)
#7-1-27	9320	9311	7	9318 (100.0%)	9385	0	9385	9385 (100.0%)

Supplementary Table

Table S3. Targeted deep-sequencing to detect InDel mutations at off-target sites using Illumina Mini-Seq. Mutations were scanned for the three lines including wild type, #3-14, and #7-1. Off-target effect was negligible except OT1 of SIDWF5-1 sgRNA_S12. This OT1 site is located on *SIDWF5-2*.

sgRNA		Total reads (raw fastq)	WT			Total reads (raw fastq)	#3-14			Total reads (raw fastq)	#7-1			
			Insertions	Deletions	Indel frequency(%)		Insertions	Deletions	Indel frequency (%)		Insertions	Deletions	Indel frequency (%)	
SIDWF5-1 sgRNA_S11	OT1	gGGAGCTTTAaCCTCtcATCTGG	55188	0	10	10 (0.0%)	48078	0	0	0 (0.0%)	54495	0	0	0 (0.0%)
	OT2	catAGCTTTATCCTCaTATCTGG	40820	0	0	0 (0.0%)	63347	0	0	0 (0.0%)	22263	0	0	0 (0.0%)
	OT3	TGGAGCTTcATCCTCagATtTGG	45434	2	2	4 (0.0%)	48846	0	4	4 (0.0%)	47858	0	2	2 (0.0%)
	OT4	TGtAGCTaaATCCTCGTATaAGG	41279	0	7	7 (0.0%)	35503	0	5	5 (0.0%)	41664	0	0	0 (0.0%)
	OT5	TGGAGgcTTATtCTCGaATCAGG	26174	0	0	0 (0.0%)	15815	0	2	2 (0.0%)	15122	0	2	2 (0.0%)
SIDWF5-1 sgRNA_S12	OT1	GCAGATTTGGcATGATaTCTTGG	32736	0	0	0 (0.0%)	48131	0	173	173 (0.4%)	21145	0	2	2 (0.0%)
	OT2	GCAGATTTGGTtTGATtTtGGG	45194	3	5	8 (0.0%)	50614	2	8	10 (0.0%)	42789	3	10	13 (0.0%)
	OT3	GaAGATTCGGTAgGATtTCTAGG	31961	0	0	0 (0.0%)	55929	0	2	2 (0.0%)	31906	0	6	6 (0.0%)
	OT4	GCAtATTTGtTATcATtTCTAGG	61779	0	6	6 (0.0%)	52921	0	3	3 (0.0%)	53101	0	3	3 (0.0%)
	OT5	GaAaATTTGcTAaGATGTCTCGG	48830	0	13	13 (0.0%)	30867	0	12	12 (0.0%)	41365	0	12	12 (0.0%)
	OT6	GtAGAcTTGGTAGGATGTcTGG	48871	0	0	0 (0.0%)	37297	0	0	0 (0.0%)	56254	0	0	0 (0.0%)

Supplementary Tables

Table S4. Oligonucleotide sequences used for amplification of the DNA flanking the target region in lettuce.

Gene	Name	Sequence	T _m (°C)
<i>LsDWF5</i>	LsDWF5_F1	CAGATGGTATACAATGGTACATCTCGATGGTTC	61
	LsDWF5_R1	GAAAATGAGTGCGGAGTATATTTCTCCCAAATGATC	61
	LsDWF5_F4	GTGGGGTTTATCTCGTCATTTCCACTATGTACC	62
	LsDWF5_R5	TCAGTAGATCCCTGGTATGATCCTATATGGAACC	62

Table S5. Oligonucleotide sequences used for realtime PCR analysis in tomato.

Gene	Name	Sequence	T _m (°C)
<i>ACTIN</i>	SIAct_qRT-PCR_F	GAGCGTGGTTACTCGTTCA	58
	SIAct_qRT-PCR_R	CTAATATCCACGTCACATTTTCAT	58
<i>SIDWF5-1</i>	SIDWF5-1_qRT-PCR_F	CGGAGACTTCTGTAGTTCCA	55
	SIDWF5-1_qRT-PCR_R	GGTGGTGTGAAAGATAGAAGAC	55
<i>SIDWF5-2</i>	SIDWF5-2_qRT-PCR_F	AGGTGCAAGTCAAAGTATGG	55
	SIDWF5-2_qRT-PCR_R	CTACTACAATACTAGAAGCAGCACT	55

Table S6. Oligonucleotide sequences used for amplification of the DNA flanking the target region in tomato.

Gene	Name	Sequence	T _m (°C)
<i>SIDWF5-1</i>	SIDWF5-1_F	GGCTCATCAGGGAACATAATAGTTGACTTCTATTGG	60
	SIDWF5-1_R2	CTCCATGCCAAGTCAAATTGG	60
	Amplicon_SIDWF5-1_F	TCGTCGGCAGCGTCAGATGTGTATAAGAGACAGACTTGTGCA	68
	Amplicon_SIDWF5-1_R	TCATCTCTGG	68
		GTCTCGTGGGCTCGGAGATGTGTATAAGAGACAGCTCACTATC	68
	AAGGACTTCAT		

Supplementary Table

Table S7. Oligonucleotide sequences used for amplification of the DNA flanking the off-target sites for NGS analysis.

sgRNA	Name	Sequence	Tm (°C)
SIDWF5-1 sgRNA_SI1	OT-1_F	CGTTGCACTCCACCCA	60
	OT-1_R	CCCCGTTTATTCTCTTGAGCT	60
	OT-2_F	GGACAGTTGAAGGAGAAGTTAGTG	60
	OT-2_R	CAACTGGGGCCATAAAGTCAATG	60
	OT-3_F	GTCGCGGCTCATAATCGAGA	60
	OT-3_R	TCATAGCAAAGTACATGGATATAGCATCAA	60
	OT-4_F	AGTCATGGTAGTTAAGTGCACCG	60
	OT-4_R	TGTCTGCGACGTCTGAGAG	60
	OT-5_F	GAGGGGAGAAAGACCCCT	60
	OT-5_R	GCTCAATGAGGCCACGAC	60
SIDWF5-1 sgRNA_SI2	OT-1_F	AGGCCTGATTTGAATCTTGACTTG	60
	OT-1_R	GGTGTCCAGTAACCTGCT	60
	OT-2_F	CGGGTCTGTTTGGATCAGTTATT	60
	OT-2_R	CTCTATAGGTTTAGCTAGCACGGA	60
	OT-3_F	GCGCCTGCTGAAATGACA	58
	OT-3_R	GTCCAGCCTAACTACCCCG	58
	OT-4_F	GGTCTCCTAAACGGAATGAGC	58
	OT-4_R	GAGTTAGGGAATGCGACGT	58
	OT-5_F	AGGGTCCTTAGAAAATACATGCAC	58
	OT-5_R	GGGAGAACTAGGGAGATGAACATTC	58
SIDWF5-1 sgRNA_SI1	Amplicon_OT-1_F	TCGTCGGCAGCGTCAGATGTGTATAAGAGACAGCACAGCTCAGTAGGTTAATCATAG	58
	Amplicon_OT-1_R	GTCTCGTGGGCTCGGAGATGTGTATAAGAGACAGCCCTGTGGGGCTACTTTTAGA	58
	Amplicon_OT-2_F	TCGTCGGCAGCGTCAGATGTGTATAAGAGACAGGGGTACAAGTGTTCGAAGAGT	58
	Amplicon_OT-2_R	GTCTCGTGGGCTCGGAGATGTGTATAAGAGACAGTCCGAAATCGGAGAACCATG	58
	Amplicon_OT-3_F	TCGTCGGCAGCGTCAGATGTGTATAAGAGACAGGACTATTGCTTTTAAATGTGCAAAATCGATTG	58
	Amplicon_OT-3_R	GTCTCGTGGGCTCGGAGATGTGTATAAGAGACAGTCATAGCAAAGTACATGGATATAGCATCAA	58
	Amplicon_OT-4_F	TCGTCGGCAGCGTCAGATGTGTATAAGAGACAGCCAGCTGGGTTGACAGA	58
	Amplicon_OT-4_R	GTCTCGTGGGCTCGGAGATGTGTATAAGAGACAGGGACCCCTCCTAAGGC	58
	Amplicon_OT-5_F	TCGTCGGCAGCGTCAGATGTGTATAAGAGACAGCCATGTCCGAGAAGCCAAAA	58
	Amplicon_OT-5_R	GTCTCGTGGGCTCGGAGATGTGTATAAGAGACAGCCCAACCCAGGTGGATATATCCCTG	58
SIDWF5-1 sgRNA_SI2	Amplicon_OT-1_F	TCGTCGGCAGCGTCAGATGTGTATAAGAGACAGGGGGATGGAGTTGTATCC TCG	58
	Amplicon_OT-1_R	GTCTCGTGGGCTCGGAGATGTGTATAAGAGACAGCCTTCATTCTCACTTTCGAGCAC	58
	Amplicon_OT-2_F	TCGTCGGCAGCGTCAGATGTGTATAAGAGACAGCATAACCAAATCAAATACTATCGGTTTTCAAAA	58
	Amplicon_OT-2_R	GTCTCGTGGGCTCGGAGATGTGTATAAGAGACAGGAATTCAAAGATGAGTAACAGTTTCTGGG	58
	Amplicon_OT-3_F	TCGTCGGCAGCGTCAGATGTGTATAAGAGACAGGGTGGAGAATACAATGTTTATTTCTCTAC	68
	Amplicon_OT-3_R	GTCTCGTGGGCTCGGAGATGTGTATAAGAGACAGGTAGTGAGTTTCTAACGAAGAAATTTGAATTC	68
	Amplicon_OT-4_F	TCGTCGGCAGCGTCAGATGTGTATAAGAGACAGGAAGCAACACTCGACGAC	68
	Amplicon_OT-4_R	GTCTCGTGGGCTCGGAGATGTGTATAAGAGACAGACCATGTACATGATGGATCATTGATC	68
	Amplicon_OT-5_F	TCGTCGGCAGCGTCAGATGTGTATAAGAGACAGCATCCTTGTACCTAACCTAGGATGG	68
	Amplicon_OT-5_R	GTCTCGTGGGCTCGGAGATGTGTATAAGAGACAGCCAAACGTCCTCCTAATTGATTAATA	68
SIDWF5-1 sgRNA_SI2	Amplicon_OT-6_F	TCGTCGGCAGCGTCAGATGTGTATAAGAGACAGCACACCAGATTTTCATGTAGATGACA	68
	Amplicon_OT-6_R	GTCTCGTGGGCTCGGAGATGTGTATAAGAGACAGCAACACACGCGCATGCATTC	68